THE NSLS-II BOOSTER DEVELOPMENT AND COMMISSIONING

V. Kiselev for the BINP and BNL teams [1]

BINP, Novosibirsk 630090, Russia

Abstract

National Synchrotron Light Source II is a third generation light source constructed at Brookhaven National Laboratory. The project includes highly optimized 3 GeV electron storage ring, linac pre-injector and full-energy injector-synchrotron. Budker Institute of Nuclear Physics has built a turnkey booster for NSLS-II. The main parameters of the booster, its characteristics and the results of commissioning are described in this paper.

INTRODUCTION

The tender on the designing, production and commissioning of the NSLS-II booster was started in January 2010. Budker Institute of Nuclear Physics won this tender in May 2010. The booster was designed, produced and delivered in full to BNL by September 2012. During 2013 the booster was assembled and all equipment was tested. The authorization to start the commissioning of the injector was received in November 2013. The BNL and BINP teams started beam injection into the Booster on December 8. The first turn was closed soon by tuning the LTB and BR orbit correctors. The beam was accelerated to 3 GeV by the end of 2013. The commissioning of the booster was successfully completed in February 2014.

BOOSTER DESIGN

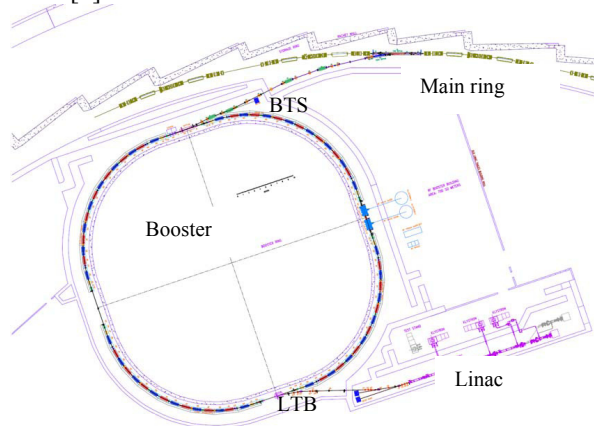The conceptual design of the booster has been done by BNL [2].

Figure 1: Schematic layout of the full energy booster.

The booster should accelerate the electron beam continuously and reliably from minimal 170 MeV injection energy to a maximal energy of 3.15 GeV and average beam current of 20 mA. The booster shall be capable of multi-bunch and single bunch operation. The main parameters of the designed booster are summarized in Table 1. The lattice provides rather low horizontal emittance of 37.4 nm·rad at the energy of extraction.

Table 1: NSLS-II Booster Main Parameters.

Energy, MeV	200	3000
Circumference, m	158.4	
Number of periods	4	
Repetition rate, Hz	1 Hz / 2 Hz	
Bunch number	1; 80-150	
RF frequency, MHz	499.68	
Betatron tunes: ν_x/ν_y	9.646 / 3.411	
Natural chromaticity: ξ_x/ξ_y	−9.5/−13.5	
Corrected chromaticity: ξ_x/ξ_y	1.25 / 2.05	
Momentum comp. factor, α	0.00882	
Hor. Emittance: ε_x, nm rad	0.17	37.4
Energy spread, σ_E/E	$0.55 \cdot 10^{-4}$	$8.31 \cdot 10^{-4}$
Energy loss per turn, U_0, keV	0.0135	685.8
Damping times: ($\tau_x \tau_s$), s	15.6; 7.8	0.0046; 0.0023

Lattice

The optical structure of the booster synchrotron consists of four quadrants. Two opposite straight sections of the ring contain elements for injection and extraction of the beam. Other two sections are intended for RF resonators and diagnostics. 60 magnets with combined functions magnetic field are set in the ring. The core of dipoles is a sector with parallel edges. For compensation of natural chromaticity of the structure the dipole magnets create sextupole component of a field. Separate quadrupole lenses provide adjustment of betatron working point during acceleration of particles and optimum acceptance of the structure. For correction of lattice chromaticity the separate sextupole lenses are inserted. Optical functions are shown in Figure 2.
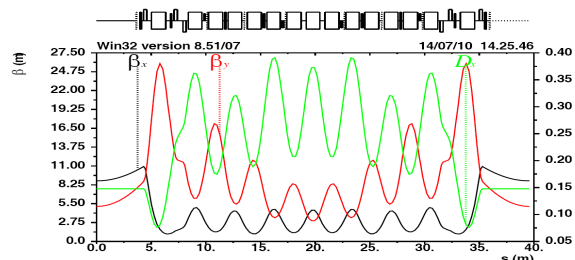

Figure 2. The betatron and dispersion functions for the lattice quadrant.

Beam Diagnostics

For successful commissioning and effective operation of the projected NSLS-II Booster, a set of beam diagnostic instruments has been designed. Fluorescent screens (8 pieces) are used for the Booster commissioning and troubleshooting. Closed orbit is measured using electrostatic BPMs (32 pieces) with turn-by-turn capability. The circulating current is measured using a DC current transformer and fill pattern by a fast current transformer. The synchrotron radiation monitor provides routine measurements of transverse beam profiles and beam sizes. Betatron tunes are measured using two pairs of striplines, the first pair is for beam excitation and the second one – for beam response measurement [3, 4].

Magnetic System

All booster magnets were made at BINP. The main parameters of the designed booster magnets are summarized in Table 2.

Table 2: Booster magnets parameters

Magnets	Total Number	Magnetic length, m	Magnetic force for 3 GeV		
			T	T/m	T/m2
BF Dipoles	28	1.24	0.46	8.2	36
BD Dipoles	32	1.30	1.13	-5.6	-43
Quadrupoles	8+8+8	0.30			20.4
Sextupoles	16	0.12			±400
Correctors	20+16	0.13	0.1		

The BINP workshop has designed and produced all dies for magnet laminations with the accuracy up to 5 µm on the critical surfaces. The BF and BD dipoles have complicated end chamfers (Fig. 3), which were chosen so as to have minimal distortion field at the extraction energy.
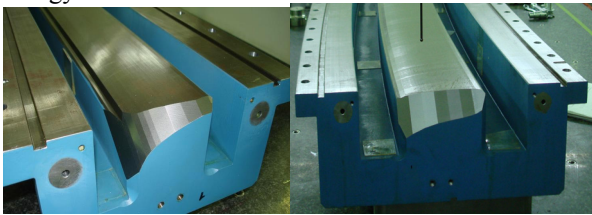

Figure 3. The BF and BD dipoles end chamfers.

The BF and BD dipole magnets were measured with the Hall sensors. The measurement method and results are described in the papers [5]. Magnetic properties of all magnets are better than the original requirements throughout the range of the energy: difference of integrated parameters between dipoles should not exceed: for integral of a field <0.1%, for integral of a gradient <0.5% and for sextupole field component <5% [6].

Injection and Extraction System

Four fast ferrite kickers and a pulse eddy-current type septum magnet are installed in the long straight section. The kicker and septum magnets are placed out of vacuum.

The booster extraction system consists of four slow orbit bumpers, AC septum, DC septum and a kicker. The main parameters of the injection and extraction system magnets are summarized in Table 3. After production, all the above-described elements were magnetically measured and long-term tested with the pulsed power supplies developed by BINP [7, 8].

All elements satisfy the requirements presented for them.

Table 3: Main parameters of IES magnets

Magnets	n	Magnetic length, m	Field T	Angle mrad	Pulse µs
Injection System for 200 MeV					
Kicker	4	0.207	0.055	17	0.3
Septum(AC)	1	0.75	0.112	125	100
Extraction System for 3 GeV					
Bump	4	0.17	0.46	7.8	1500
Kicker	1	0.83	0.073	6.1	0.3
Septum(AC)	1	0.6	0.8	48	150
Septum(DC)	1	1.2	0.89	106	-

COMMISSIONING

Thanks to the good quality of the booster magnets and precise booster alignment, commissioning of the booster passed without any problems. The first turn was closed soon by tuning the LTB and BR orbit correctors. The beam was monitored using the beam flags and BPMs in the single-pass mode. After achievement of the captured beam, the orbit at injection was corrected and the beam was accelerated. The diagram represents the measurements of the orbit during acceleration. The force of correctors during ramping was not changed (Fig. 4).
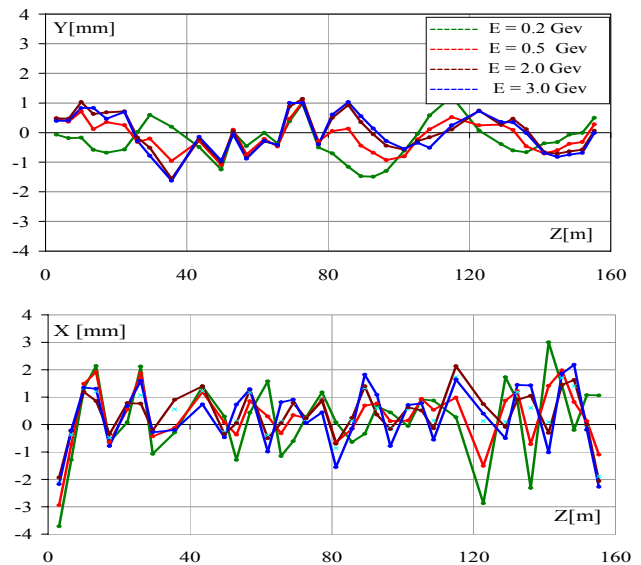

Figure 4. Vertical and horizontal orbit of beam along the whole ramp.

As can be seen from Figure 4, the beam orbit remains constant during the ramp with accuracy of ± 1 mm in the vertical plane and ± 2 mm in the horizontal without additional correction.

Thereafter the optical model of the magnetic structure was improved towards better booster ring parameters using the data of the final booster survey and the results from beam position monitors. The optical functions and betatron tunes were corrected throughout the ramp. As a result, the betatron frequences over the entire ramp remained constant (Fig. 5).
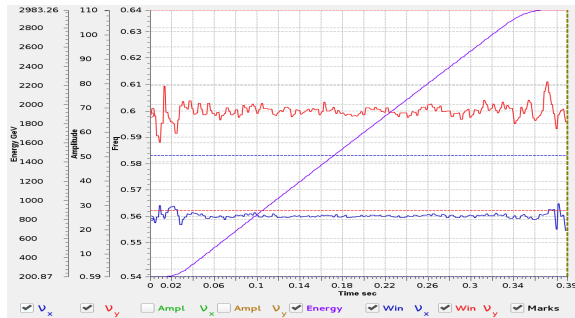

Figure 5: The horizontal (blue) and vertical (red) tunes along the whole ramp (purple).

This reduced beam losses during the ramp to below 5%. Besides, an additional adjustment of the optical functions of the linac-to-booster transport line was carried out, which resulted in increasing efficiency of particle capture and acceleration up to ~ 95 % (Fig.6).
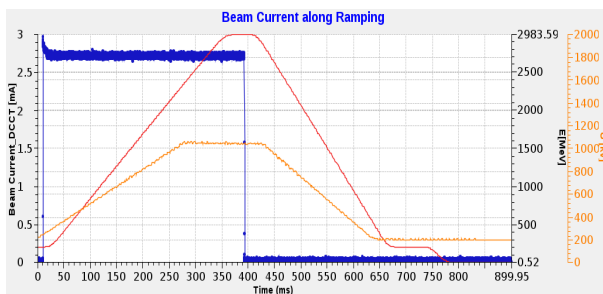

Figure 6: The beam current from DCCT (blue), the beam energy according dipole magnet currents (red) and the RF cavity voltage (orange) during 1Hz-cycle.

Emittance Measurement

Emittance value was derived from a spot of the synchrotron light [9]. The BR-A1SLM output port is located close to the DS straight section, in a region with minimal dispersion. Synchrotron light is emitted from the BR-A1BD8 dipole magnet. Using operating machine currents, Twiss parameters at the source are estimated to be β_x = 5.8 m, β_y = 23.8 m, and η_x=0.1 m. At extraction energy the measured emittances were ε_x=33 nm and ε_y=4nm.

The transverse stability of extracted beam was checked. Beam position stability was measured using the flag disposed in the extraction channel (BTS). Transverse

beam stability better than ± 30 μm was observed at the repetition rate of 1 Hz during 1 hour.
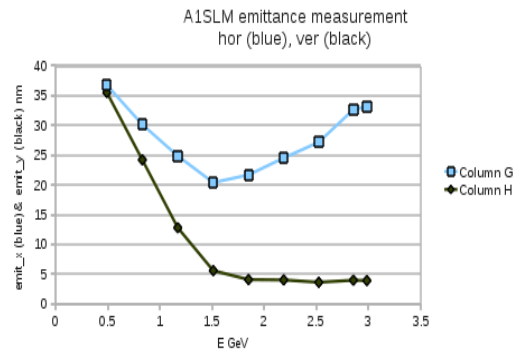

Fig. 7. Horizontal and vertical emittance during the acceleration cycle as determined by the profile of the synchrotron light seen by the BR-A1SLM monitor.

CONCLUSION

The NSLS-II 3-GeV booster synchrotron has passed the acceptance testing and the machine performance closely corresponds to the project requirements. The booster is a robust machine that will be an effective injector for the NSLS-II storage ring. The booster commissioning was successfully completed in February 2014. All booster systems work according to the design. The commissioning of NSLS-II Storage Ring was started in March 2014 and stored beam was achieved on April 5, 2014.

REFERENCES

[1] **BINP team**: A.Akimov, O.Anchugov, A.Batrakov, O.Belikov E.Bekhtenev, P.Cheblakov, A.Chernyakin A.Derbenev, A. Erokhin, S.Gurov, S.Karnaev, G.Karpov, R. Kadyrov, V.Kiselev, V.Kobets, V.Konstantinov, V.Kolmogorov, A.Korepanov, E.Kuper, V.Kuzminykh, E.Levichev, V.Neyfeld, I.Okunev, V.Petrov, M.Petrichenkov, A.Polyansky, D.Pureskin, A.Rakhimov, S.Ruvinskiy, T.Rybitskaya, L.Schegolev, A.Semenov, D.Senkov, S.Serednyakov, S.Shiyankov, D.Shvedov, S.Sinyatkin, A.Sukhanov, A.Zhuravlev

BNL New York, USA team: G.Bassi, A.Blednykh, E.Blum, W.Cheng, J.Choi, J.De Long, R.Fliller, F.Gao, W.Guo, Y.Hidaka, S.Kramer, S.Krinsky, Y.Li, M.Maggipinto, D.Padrazo, B.Podobedov, J.Rose, S.Seletskiy, O.Singh, V.Smaluk, T.Shaftan, W.Wahl, G.Wang, F.Willeke, L.Yang, X.Yang, L.Yu, E.Zitvogel, P.Zuhoski.

[2] T.Shaftan et al., NSLS-II Tech. note 0061 (2009).
[3] V.Smalyuk et al., DIPAC'11, MOPD01, p. 29 (2011).
[4] E.Bekhtenev et al., RUPAC'12, WEPPD029, (2012).
[5] I. Okunev et al., IPAC'13, THPME032, p. 3579 (2013).
[6] S.Sinyatkin et al., IPAC'13, THPME029, p. 3570 (2013).
[7] A. Zhuravlev et al., IPAC'13, THPME033, p. 3582 (2013).
[8] D. Shvedov et al., IPAC'13, THPME033, p. 717 (2013).
[9] S.Gurov et al., IPAC'14, MOPRO088, (2014).